Integrating Viability Information into a Cardiac Model for Interventional Guidance*

Helko Lehmann[1], Reinhard Kneser[1], Mirja Neizel[2], Jochen Peters[1], Olivier Ecabert[1], Harald Kühl[2], Malte Kelm[2], and Jürgen Weese[1]

[1] Philips Research Laboratories, Aachen, Germany
[2] Medical Clinic I, University Hospital of the RWTH Aachen, Germany

Abstract. It has been demonstrated that 3D anatomical models can be used effectively as roadmaps in image guided interventions. However, besides the anatomical information also the integrated display of functional information is desirable. In particular, a number of procedures such as the treatment of coronary artery disease by revascularization and myocardial repair by targeted cell delivery require information about myocardial viability. In this paper we show how we can determine myocardial viability and integrate the information into a patient-specific cardiac 3D model. In contrast to other work we associate the viability information directly with the 3D patient anatomy. Thus we ensure that the functional information can be visualized in a way suitable for interventional guidance. Furthermore we propose a workflow that allows the nearly automatic generation of the patient-specific model. Our work is based on a previously published cardiac model that can be automatically adapted to images from different modalities like CT and MR. To enable integration of myocardial viability we first define a new myocardium surface model that encloses the left ventricular cavity in a way that suits robust viability measurements. We modify the model-based segmentation method to allow accurate adaptation of this new model. Second, we extend the model and the segmentation method to incorporate volumetric tissue properties. We validate the accuracy of the segmentation of the left ventricular cavity systematically using clinical data and illustrate the complete method for integrating myocardial viability by an example.

Keywords: Scar tissue, papillary muscles, endocardial trabeculae, model-based segmentation, late enhancement, MRI, cardiac, interventional guidance.

1 Introduction

While the real-time images acquired during an image guided intervention such as a revascularization procedure provide some means for orientation and navigation they often do not display all the information required for therapeutic decisions and outcome control. In [4] and [9] it has been demonstrated that many interventions may benefit

* The research leading to these results has received funding from the European Community's Seventh Framework Programme (FP7/2007-2013) under grant agreement n° 224495 (euHeart project).

N. Ayache, H. Delingette, and M. Sermesant (Eds.): FIMH 2009, LNCS 5528, pp. 312–320, 2009.

from the display of an accurate anatomical 3D model as an overlay on the fluoroscopy image stream. However, besides the anatomical information the display of additional functional information is often desirable. For example, an infarcted myocardial region can only regenerate following a revascularization of the blood supplying coronary arteries if sufficient viable tissue is present in the region [6]. Similar viability information is required for myocardial repair, where drugs or cells are applied targeted to the infarcted tissue.

In this paper we show how we can determine myocardial viability and integrate the information into a patient-specific cardiac 3D model suitable for interventional guidance. To increase efficiency and to decrease inter-observer variability we propose a workflow that allows fully automatic generation of the patient-specific cardiac model and semi-automatic integration of viability information. Our approach requires the following application-specific extensions of the general comprehensive cardiac model of [3] and [8]:

- As motivated in [7], to increase the robustness of the viability estimation, we systematically exclude the endocardial trabeculae and papillary muscles from the myocardium model of [8]. Furthermore, we extend the segmentation process to interpolate a smooth surface in areas of the myocardium where these structures are attached.
- To provide the functional information in a way that is suitable for image guided interventions we associate the viability information directly with the 3D patient anatomy represented by the cardiac model. To this end we extend the part of the model describing the myocardium by a volumetric mesh. Other methods have been developed for visualization and diagnosis of viability [5] [12]. However in contrast to our approach they do not maintain the 3D anatomical context and are therefore less suitable for interventional guidance.
- To integrate the viability information, we adapt the cardiac model to a whole heart 3D MRI data set that matches a late enhancement 3D MRI data set of the same patient (similar approach to [2] for cine data). Thereby we avoid an additional segmentation step of the ill-defined myocardium contours in the late enhancement data. We finally employ a gray-value thresholding method to classify volumetric mesh elements representing myocardium tissue into viable and non-viable.

The paper is structured as follows. In Section 2 we describe the workflow from data acquisition to a patient-adapted integrated model for interventional guidance. In Section 3 our technical extensions to the cardiac model and the associated model-based segmentation process of [3] and [8] are described in detail. We validate the improved myocardium segmentation in Section 4 and illustrate the complete method by an example. In Section 5 we conclude and give an outlook on the next steps and other applications of the cardiac model.

2 Clinical Workflow

An MRI study of a patient with suspected acute myocardial infarction consists of a number of different imaging steps to establish both anatomy and function. For our approach we assume that the patient is undergoing a non-contrast enhanced

steady-state free-precession scan of the whole heart (WH) to examine anatomical properties. To determine myocardial viability a 3D late enhancement (LE) technique with phase sensitive inversion recovery (PSIR) is employed (see Fig. 1). During the image acquisitions it is ensured that both the whole heart image and the LE image are acquired in the same heart phase and breathing phase by employing a navigator technique. Thereby misregistrations between the WH image and the LE image due to heart motion and respiratory motion can be avoided.

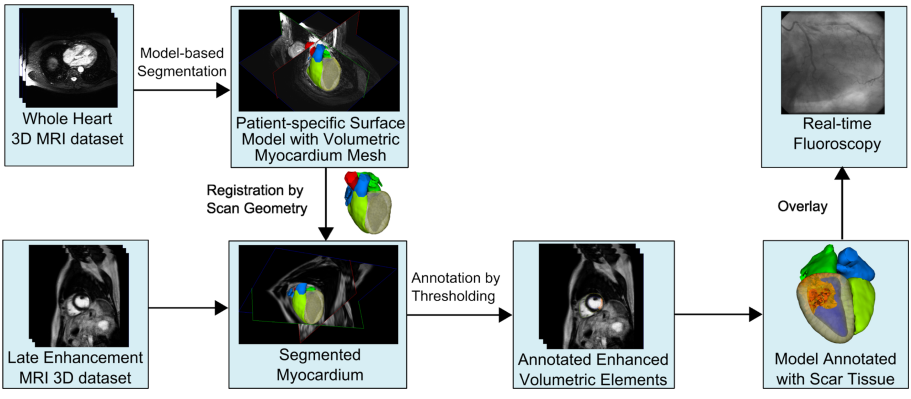

Fig. 1. Illustration of the workflow

The acquired whole heart data set is automatically segmented using a comprehensive cardiac surface model where the myocardium component comprises additionally a fine volumetric mesh of tetrahedrons. The resulting adapted model represents the patient's cardiac anatomy as well as a complete covering of the myocardium by volumetric mesh elements. Since the WH image and the LE image have been acquired in the same heart phase and breathing phase, the model adapted to the WH image can be mapped to the LE image using the common patient coordinate system. However, misalignments between the WH image and the LE image are possible and can be primarily attributed to patient movement. They can be corrected in an additional registration step if required. Mapping of the model results in a segmentation of the myocardium and the left ventricular (LV) cavity in the LE image. Then the volumetric mesh elements of the myocardium model are annotated if the contained voxels in the LE image are classified as scar tissue. Since in LE images the scar tissue appears hyperintense in contrast to dark normal myocardium tissue, voxels in the LE image can be classified as scar if they exceed a certain intensity threshold. Here we assume this threshold to be manually selected. The annotated model is finally displayed during intervention, e.g. as an overlay over a real-time fluoroscopy image.

3 Integration of Scar Tissue Information into a Cardiac Model

In the above described workflow we rely heavily on the segmentation of the heart in the WH image as described in [3] and [8]. However our envisioned application requires specific improvements, which we describe in this section.

3.1 Model-Based Whole Heart Segmentation

The essential idea of the model-based segmentation of [3] and [8] is to adapt a triangular surface mesh to an image while additionally considering a shape constraint. The adaptation is performed by iterating a boundary detection step and a mesh deformation step.

During the boundary detection step for each mesh triangle i a new target point x_i^{target} is searched in the neighborhood of the current location by maximizing a triangle specific image feature response function. At the same time a reliability function w_i is computed which increases with the feature response and decreases with the distance of the target point to the original triangle. During the mesh deformation step the mesh is modified such that

$$E_{tot} = \underbrace{\sum_{i=1}^{V} \sum_{j \in N(i)} \sum_{k=1}^{K} \omega_{i,k} ((v_i - v_j) - (T_k[m_i] - T_k[m_j]))^2}_{E_{int}} + \alpha \cdot \underbrace{\sum_i w_i \cdot D(x_i^{target}, c_i)^2}_{E_{ext}} \tag{1}$$

is minimized.

The shape constraint is modeled by the internal energy function E_{int}, which increases if the vector $(v_i - v_j)$ between a model point with index i and a neighboring model point with index $j \in N(i)$ deviates from the corresponding vector of a transformed mean shape. The respective transformation models the variability of the mean shape m_i and is defined via the affine transformations $T_k[m_i]$ and the weights $\omega_{i,k}$. The external energy E_{ext} describes how well the mesh fits to the image. To this end, for all triangles i the deviations D of the triangle center c_i from the corresponding image target point x_i^{target} of the boundary detection step are accumulated.

While the mean shape is determined from a set of reference meshes the image feature response functions are learned from a set of reference meshes with corresponding images, for details see [3]. In the following we refer to a model as a triangle mesh together with the associated image feature response functions.

3.2 Robust Model-Based Myocardium Segmentation

To quantify scar tissue in the myocardium an accurate distinction of the myocardium tissue from the LV cavity is required since in LE images the intensity of the LV blood pool is very similar to contrast enhanced scar tissue in the myocardium. However, the exact segmentation of the blood pool from other tissue in WH images is difficult and may result in large inter-observer variability as small structures such as trabeculae and papillary muscles cannot be accurately identified. More robust results can be achieved by considering trabeculae and papillary muscles to be part of the LV cavity during segmentation [7]. To achieve similar robust results using model-based segmentation we follow this approach and modify the model M_{Ref} and adaptation of [8] accordingly.

The segmentation model is the result of an automatic learning process based on image data annotated with reference meshes. Therefore, as a first step we modify these meshes such that, in contrast to the reference meshes used to train the model M_{Ref}, the submesh representing the LV cavity encloses all the trabeculae and papillary muscles (see Fig. 2). Based on the new reference meshes both the mean shape model and the new image feature response functions are learned, resulting in the new cardiac model M_{PT}.

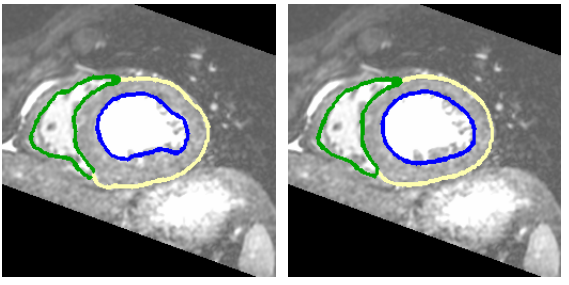

Fig. 2. Reference meshes used to train models M_{Ref} (left) and M_{PT} (right)

However, adapting the model M_{PT} to image data still results in larger deviations of the adapted meshes to the desired segmentation result, particularly in areas where trabeculae and papillary muscles are attached to the myocardium. This is due to the fact that in these areas boundaries are searched and detected although the segmentation cannot be supported by boundaries in the image.

Based on the assumption that trabeculae and papillary muscles distract the segmentation only in certain areas of the left ventricle, we identify these critical regions automatically during the model training and modify the segmentation process to rely in critical regions on the shape model. More precisely, we first use the model M_{PT} to segment the training images and calculate from this segmentation for each triangle of the model and each image the error as the distance between the reference triangle and the adapted triangle (see Fig. 3a). If this distance is larger than some threshold T_d the segmentation at this triangle is regarded as unreliable in the particular image. A triangle of the model is defined as *critical* if it was classified as unreliable for at least T_N training images (the resulting critical triangles for suitable parameters are highlighted in Fig. 3b).

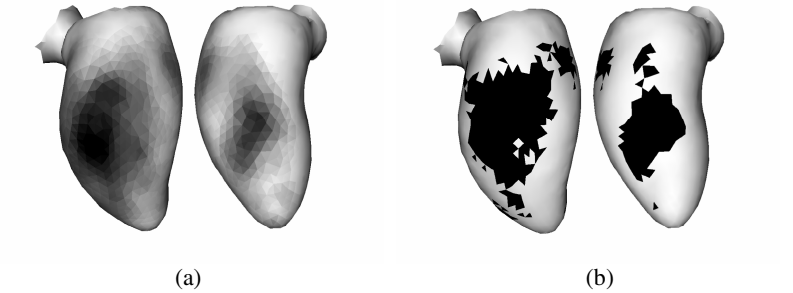

(a) (b)

Fig. 3. a) Mean error over all images (large error dark) b) Critical triangles (dark)

To allow for the accurate adaptation of critical triangles the model-based segmentation procedure is extended by performing two different iteration cycles instead of one. During the deformation step of the first cycle the influence of the boundary detection is disabled for all critical triangles by setting w_i in (1) to 0. Thereby critical triangles are geometrically interpolated from neighboring triangles only based on the

shape model. During the deformation step of the second cycle, w_i is determined as in [8] for all triangles but the boundary detection step is modified to detect boundaries only in a very small neighborhood of each triangle. Hence, both critical as well as non-critical triangles may adapt to nearby image boundaries, e.g. if a boundary is present in the current image that has not been reliably present in the training data.

3.3 A Volumetric Mesh for the Myocardium

The meshes in M_{Ref} and M_{PT} are surface meshes that allow vertices, edges and triangles to be annotated and used for quantification of geometrical properties such as a distance between anatomical landmarks and the surface area of a sub-mesh. We may also represent a tissue type as the volume enclosed by a surface mesh if the tissue types can be separated by a well defined surface. However, if the tissue types are not separable in this way, such as viable and non-viable myocardium tissue, other means have to be considered. Hence, to enable classification and representation of these tissue types we propose to cover the volume enclosed by the myocardium surface with a volumetric mesh of tetrahedrons.

Since the covering of the myocardium volume with a volumetric mesh is not driven by image characteristics but only shape characteristics of the myocardium surface, the volumetric mesh should not influence the result of the surface adaptation. Hence, to enable integration with the model-based segmentation the volumetric mesh must fulfill the surface constraints of the myocardium, i.e. surface vertices and edges must not be altered. Thereby, no new points (*Steiner points*) should be generated on the myocardium surface, i.e. additional vertices may only be introduced within the volume of the myocardium. To allow a homogeneous resolution of the tissue characterization the volume elements should be similar in size and approximately regular.

Furthermore, a correspondence between volumetric mesh elements of cardiac models adapted to different patients is desirable, as it allows a mapping of volumetric mesh elements to standard anatomical regions of the myocardium, e.g. according to the American Heart Association [1]. Consequently, we generate the volumetric mesh only once for the mean model by constrained Delaunay tetrahedralization [11]. During the adaptation of the mean model to the patient image data, first the surface model is deformed as explained in Section 3.2. Second, the deformation of the volumetric mesh is performed by interpolating the vertex coordinates of all vertices located inside the myocardium from the vertex coordinates on the myocardium surface. This is realized by interpolating for each Steiner point a transformation from the transformations T_k computed for the adapted surface. Then, the external energy in equation (1) is set to 0, the vertex coordinates of surface points in the internal energy term are fixed to the values resulting from the surface adaptation, and the resulting (internal) energy function is minimized for the Steiner points only.

4 Results

We evaluate the improved segmentation of the left ventricle on 43 WH images acquired from ischemic disease patients to inspect the coronary arteries. The images

have been acquired on Philips Intera and Achieva 1.5T scanners at end-diastolic phase over various cardiac cycles and breathing compensated. For all 43 data sets manually corrected reference meshes have been created enclosing the trabeculae and papillary muscles in the LV cavity as described in Section 3.2. A subset of 20 of these reference meshes have been created with special care by averaging the annotations of 5 technical and clinical experts. These datasets serve in the following as ground truth. Image feature response functions are trained using all 43 images and remain unchanged for all experiments. The other components of the models, i.e. the respective mean shape and critical triangle set are trained and evaluated on the subset of 20 patients in a leaving-one-out fashion using respectively one data set for evaluation and 19 sets for training. Evaluation is performed by comparing the automatically adapted meshes to the ground truth meshes. Both the symmetrized mean Euclidean "surface-to-patch" distance as described in [8], averaged over all triangles of the left ventricle, and the distribution of these distances serve as error measures. They are shown in Table 1.

We compare the three models M_{Ref}, M_{PT}, M_{PT} + *2 cycle segm*. The models M_{Ref} and M_{PT} are both trained in the same setup where the only difference is that the old uncorrected reference meshes are used to train M_{Ref} while M_{PT} is trained using the new reference meshes enclosing the trabeculae and papillary muscles in the LV cavity. For M_{PT} + *2 cycle segm* critical triangles are determined automatically and additional segmentation cycles are added as described in Section 3.2.

Note that for a large range of values for the parameters defining the set of critical triangles similar errors can be obtained. We achieved best results using $T_d = 0.8$mm and $T_N = 15$. These parameters are also used to generate the error values presented in Table 1 and Fig. 3b.

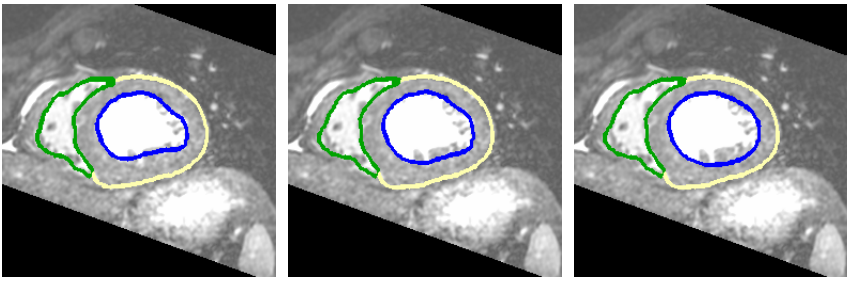

Fig. 4. Typical segmentation results (left to right: M_{Ref}, M_{PT}, M_{PT} + *2 cycle segm*)

Typical segmentation results are displayed in Fig. 4. The experiments show that the adapted model M_{Ref} inaccurately follows trabeculae and papillary muscles resulting in a mean error of 0.75 mm and a large amount of distant triangles. The distances decrease if model M_{PT} is used but the segmentation results are still unsatisfying. The model M_{PT} + *2 cycle segm* provides good results, both in terms of error and from visual inspection.

Table 1. Mean errors and distribution for the left ventricle

Model/Segm.	Mean Error (mm)	Percentage of Triangles with error range (%)		
		< 1.0 mm	1.0 – 2.0 mm	> 2.0 mm
M_{Ref}	0.75	69.7	29.3	1.0
M_{PT}	0.65	83.1	16.9	0.0
M_{PT} + *2 cycle segm.*	0.56	97.4	2.6	0.0

To illustrate the annotation of viability information in the new cardiac model we follow the workflow described in Section 319. To classify myocardial tissue into viable and non-viable we employ a simple thresholding algorithm. Thereby the tissue covered by a tetrahedron is considered non-viable if a number of samples acquired within the volume of the tetrahedron have intensities larger than a manually adjusted threshold (see Fig. 5).

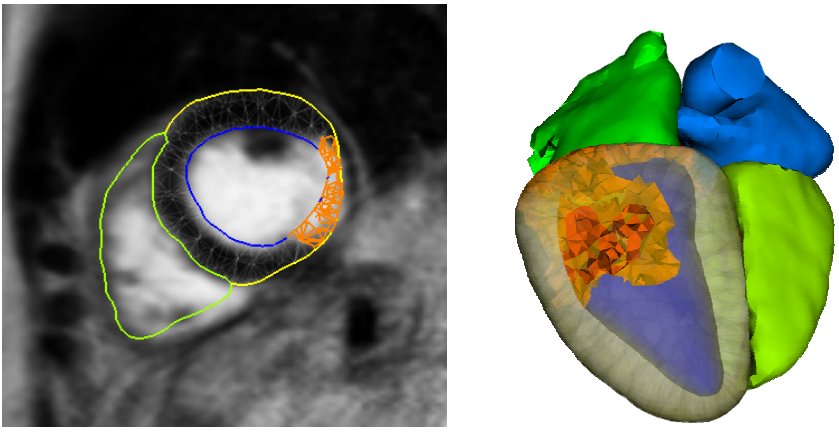

Fig. 5. A cut through the model-annotated LE data (left) and the model (right)

5 Conclusion

We have presented a workflow that allows the integration of viability information into a patient-specific cardiac model. By associating the viability information directly with the 3D patient anatomy we ensure that the model is suitable for interventional guidance, e.g. for revascularization procedures as a roadmap overlaying a real-time fluoroscopy stream.

As we aim to generate the model automatically we have extended a model-based segmentation method for the heart. In particular, we have improved the segmentation of the myocardium tissue in whole heart MR images to allow more robust automatic delineation of myocardium tissue. We have validated the improvements using clinical data from patients with ischemic disease. Furthermore, we have integrated the automatic adaptation of a volumetric mesh covering the myocardium into the segmentation process. We have shown how this volumetric mesh is used to associate functional information such as viability with the patient-specific anatomical model. Thereby we have demonstrated that we can perform viability measurements based on

a mapping of the patient-specific model to an appropriate 3D late enhancement data set and the application of a threshold-based method.

For clinical use, an improved registration between the adapted cardiac model and the LE image may be required. Furthermore the manual threshold used to differentiate between non-viable and viable tissue may be replaced by an automatic tissue classification. Future work may also address the integration of further information such as myocardial perfusion data and supply territories into the cardiac model.

The volumetric mesh model of the myocardium can also be used to perform biomechanical simulations, if mechanical properties are associated with each volumetric element

Acknowledgements

We thank M. Breeuwer, P. Ermes, G. Hautvast, F. Gerritsen of Philips Medical Systems Healthcare Informatics (Best, The Netherlands) for providing MR data and modified ground truth.

References

1. Cerqueira, M.D., et al.: Standardized myocardial segmentation and nomenclature for tomographic imaging of the heart: A statement for healthcare professionals from the Cardiac Imaging Committee of the Council on Clinical Cardiology of the American Heart Association. J. of the American Society of Echocardiography: official publication of the American Society of Echocardiography 15(5), 463–467 (2002)
2. Dikici, E., O'Donnell, T., Setser, R., White, R.D.: Quantification of Delayed Enhancement MR Images. In: Barillot, C., Haynor, D.R., Hellier, P. (eds.) MICCAI 2004. LNCS, vol. 3216, pp. 250–257. Springer, Heidelberg (2004)
3. Ecabert, O., et al.: Automatic Model-Based Segmentation of the Heart in CT Images. IEEE Trans. Med. Imaging 27(9), 1189–1201 (2008)
4. Gutiérrez, L.F., et al.: Technology Preview: X-ray Fused With Magnetic Resonance During Invasive Cardiovascular Procedures. Catheterization and Cardiovascular Interventions 70(6), 773–782 (2007)
5. Hennemuth, A., et al.: A Comprehensive Approach to the Analysis of Contrast Enhanced Cardiac MR Images. IEEE Trans. Med. Imaging 27(11), 1592–1610 (2008)
6. Kim, R.J., et al.: The Use of Contrast-Enhanced Magnetic Resonance Imaging to Identify Reversible Myocardial Dysfunction. N. England J. Med. 343(20), 1445–1453 (2000)
7. Papavassiliu, T., et al.: Effect of Endocardial Trabeculae on Left Ventricular Measurements and Measurement Reproducibility at Cardiovascular MR Imaging. Radiology 236(1), 57–64 (2005)
8. Peters, J., et al.: Automatic Whole Heart Segmentation in Static Magnetic Resonance Image Volumes. In: Ayache, N., Ourselin, S., Maeder, A. (eds.) MICCAI 2007, Part II. LNCS, vol. 4792, pp. 402–410. Springer, Heidelberg (2007)
9. Rhode, K.S., et al.: A system for real-time XMR guided cardiovascular intervention. IEEE Trans. Med. Imaging 24(11), 1428–1440 (2005)
10. Sermesant, M., et al.: Cardiac function estimation from MRI using a heart model and data assimilation: Advances and difficulties. Medical Image Analysis 10(4), 642–656 (2006)
11. Si, H., Gaertner, K.: Meshing Piecewise Linear Complexes by Constrained Delaunay Tetrahedralizations. In: Proc. of the 14th International Meshing Roundtable, pp. 147–163 (2005)
12. Termeer, M., et al.: CoViCAD: Comprehensive Visualization of Coronary Artery Disease. IEEE Trans. Vis. Comput. Graph 13(6), 1632–1639 (2007)